The Cryosphere Discuss., 7, 1177–1213, 2013
www.the-cryosphere-discuss.net/7/1177/2013/
doi:10.5194/tcd-7-1177-2013

The Cryosphere Discussions

Open Access

Discussion Paper | Discussion Paper | Discussion Paper | Discussion Paper |

Predicting subglacial lakes and meltwater drainage pathways beneath the Antarctic and Greenland ice sheets

S. J. Livingstone[1], C. D. Clark[1], and J. Woodward[2]

[1]Department of Geography, University of Sheffield, Sheffield, S10 2TN, UK
[2]Department of Geography, Engineering and Environment, Northumbria University, Newcastle-Upon-Tyne, NE1 8ST, UK

Received: 5 March 2013 – Accepted: 6 March 2013 – Published: 21 March 2013

Correspondence to: S. J. Livingstone (s.j.livingstone@sheffield.ac.uk)

Published by Copernicus Publications on behalf of the European Geosciences Union.

Abstract

In this paper we use the Shreve hydraulic potential equation to predict subglacial lakes and meltwater drainage pathways beneath the Antarctic and Greenland ice sheets. For the Antarctic Ice Sheet we are able to predict known subglacial lakes with a >70 % success rate, which demonstrates the validity of this method. Despite the success in predicting known subglacial lakes the calculations produce two-orders of magnitude more lakes than are presently identified, covering 4 % of the ice-sheet bed. The difference is thought to result from our poor knowledge of the bed (which has resulted in artefacts associated with the interpolation method), intrinsic errors associated with the simplified modelling approach and because thousands of subglacial lakes, particularly smaller ones, remain to be found. Applying the same modelling approach to the Greenland Ice Sheet predicts only 90 lakes under the present-day ice-sheet configuration, covering 0.2 % of the bed. The paucity of subglacial lakes in Greenland is thought to be a function of steeper overall ice-surface gradients. As no lakes have currently been located under Greenland, model predictions will make suitable targets for radar surveys of Greenland to identify subglacial lakes. During deglaciation from the Last Glacial Maximum both ice sheets had more subglacial lakes at their beds, though many of these lakes have persisted to present conditions. These lakes, inherited from past ice-sheet configurations would not form under current surface conditions, suggesting a retreating ice-sheet will have many more subglacial lakes than an advancing ice sheet. This hysteresis effect has implications for ice-stream formation and flow, bed lubrication and meltwater drainage. The lake model also allows modelling of the drainage pathways of the present-day and former Greenland and Antarctic ice sheets. Significantly, key sectors of the ice sheets, such as the Siple Coast (Antarctica) and NE Greenland Ice Stream system, are shown to have been susceptible to drainage switches and capture by neighbouring networks during deglaciation thus far.

TCD

7, 1177–1213, 2013

1 Introduction

Understanding the drainage of meltwater beneath ice is fundamental to resolving ice-flow dynamics because water pressure influences both the strength of the subglacial sediment and the frictional interaction between ice and its sole (Clarke, 2005; Schoof, 2010). However, subglacial meltwater drainage is dynamic in space and time and varies in a complicated manner coupled to ice mechanics (e.g. Bartholomew et al., 2010). Possible meltwater networks at the ice-bed interface are thought to include: (i) discrete tunnel systems (e.g. Röthlisberger, 1972; Walder and Hallet, 1979; Nienow et al., 1998); (ii) distributed networks of passageways and cavities (e.g. Lliboutry, 1979; Kamb, 1987; Sharp et al., 1989); (iii) thin water films (e.g. Hallet, 1979; Lappegard et al., 2006); and (iv) Darcian flow through sediments (e.g. Hubbard et al., 1995). These drainage configurations evolve on daily to millennial time-scales as basal conditions are perturbed (Hubbard et al., 1995; Bartholomew et al., 2010).

The identification of subglacial lakes beneath the Antarctic Ice Sheet (AIS) (Robin et al., 1970) has altered our perception of how meltwater drains and is stored beneath large ice masses (e.g. Smith, 2009). Indeed, subglacial lakes beneath the AIS are now known to comprise a crucial component of the subglacial environment, capable of actively interacting with the surrounding hydrological network and transmitting large volumes of meltwater between lakes and towards the grounding-line (e.g. Wingham et al., 2006; Fricker et al., 2007; Smith, 2009). An inventory of over 380 known subglacial lakes has been compiled recently for the AIS (Wright and Siegert, 2011), and thus, unlike the subglacial hydrological system as a whole (i.e. the pathways and networks), we have a decent (and rapidly improving) understanding of the spatial distribution and geometry of subglacial lakes. They are therefore a valuable resource for constraining and testing glacial models (Pattyn, 2010).

Despite conceptual breakthroughs in how we understand subglacial hydrology, relatively little is known about the distribution of water and the form of the drainage system. And although subglacial lakes are being identified beneath the AIS, they have only been posited under other (palaeo-)ice sheets (e.g. Livingstone et al., 2012). One method of investigating the subglacial hydrological network is to calculate the hydraulic potential from the bed and ice-surface topographies (Shreve, 1972), and then to use simple routing techniques to derive meltwater flowpaths and subglacial lakes (e.g. Evatt et al., 2006; Siegert et al., 2007; Wright et al., 2008). This method has potential application in predicting and investigating subglacial hydrological systems in both contemporary and palaeo- settings and it is therefore important to verify how well hydrological calculations replicate known subglacial drainage configurations.

In this paper, subglacial meltwater drainage pathways and lakes are calculated both for the present-day Antarctic and Greenland ice sheets, and over the last 20 000 yr of their evolution. The inventory of subglacial lakes for the AIS (Wright and Siegert, 2011) is used to test whether the hydrological potential can be used to predict the pattern of known subglacial lakes. In particular, because the ice thickness and bed topography are delimited from radar data that uses the subglacial lake-surface reflector, the hydrological potential surface will include known lakes. This may consequently preclude their identification. If known subglacial lakes can be predicted the simulated subglacial lakes will allow us to simulate locations where subglacial lakes have not been observed, both beneath the Antarctic and Greenland ice sheets. Derived subglacial meltwater flowpaths provide information on hydrological connections, the structure of the drainage system and their association with ice-stream corridors (see Siegert et al., 2007, for a similar approach). Subglacial meltwater pathways and lakes calculated at time-slices through the deglaciation thus far, of both the Antarctic and Greenland ice sheets, allow an assessment of the sensitivity of subglacial hydrological pathways and subglacial lakes to ice-sheet evolution (e.g. Wright et al., 2008). This has allowed us to speculate on the likely changes in subglacial lake formation and drainage during the last deglaciation, and to predict what may happen in the future.

TCD
7, 1177–1213, 2013

2 Methods

2.1 Calculating subglacial water flow and storage

The flow and storage of meltwater under ice masses is principally governed by the hydraulic potential (Φ), which is a function of the elevation potential and water pressure (Shreve, 1972):

$$\Phi = \rho_w g h + \mathrm{Pw} \tag{1}$$

where ρ_w is the density of water ($1000\,\mathrm{kg\,m^{-3}}$), g is the acceleration due to gravity, h is the bed elevation and Pw is the water pressure. The water pressure is a function of the ice overburden pressure and effective pressure:

$$\mathrm{Pw} = F(\rho_i g H) \tag{2}$$

where ρ_i is the density of ice ($917\,\mathrm{kg\,m^{-3}}$), H is the ice thickness and F is the flotation criterion, which describes the effective pressure as a ratio of subglacial water pressure, Pi, to the ice-overburden pressure, Pw ($F = \mathrm{Pw}/\mathrm{Pi}$). Understanding the spatial and temporal distribution of basal meltwater pressure at the ice-bed interface is non-trivial and depends on the underlying geology, and (changes in) the configuration of the drainage system, basal ice temperature and ice-overburden pressure (Clarke, 2005). However, limited borehole observations show that Pw is close to the ice overburden pressure ($F > 0.95$, (e.g. Kamb, 2001) and therefore an assumption can be made that $F = 1$ (effective pressure is zero), allowing us to re-write Eq. (1) as:

$$\Phi = \rho_w g h + \rho_i g H \tag{3}$$

If we assume the ice sheet was wholly warm-based and that basal melting and effective pressure were uniformly spread, Eq. (3) can be used to compute a three-dimensional surface of the hydraulic potential at the ice-sheet bed from Digital Elevation Models

TCD
7, 1177–1213, 2013

(DEMs) of the ice and bed surface topographies. Because meltwater should follow the maximum gradient of the hydraulic potential surface, simple routing mechanisms in a GIS (ArcMap) can be used to simulate meltwater pathways and to identify locations of hydraulic minima where subglacial lakes may develop (e.g. Evatt et al., 2006; Siegert et al., 2007; Wright et al., 2008). It is also possible to arbitrarily investigate the sensitivity of subglacial lakes and meltwater pathways to uniform increases in effective pressure, by modifying the F-fraction in Eq. (2) accordingly.

Equation (3) can be re-arranged to demonstrate the well-known result that the contribution of the ice-surface gradient to the hydraulic potential is a factor of ≈ 10 times that of the bed gradient. Thus, the ice-surface, which is capable of rapid changes in ice elevation and slope, is the primary driver of subglacial water. However, the weaker influence of the bed is partially offset by its greater relief and spatial variability (Wright et al., 2008).

2.2 Antarctic datasets and statistics

Ice-surface and bed topographies were taken from the new BEDMAP2 dataset, which is interpolated from 25 million measurements and constructed at 1 km resolution (Fretwell et al., 2013). In addition, BEDMAP2 was re-gridded at 5 and 10 km to explore the effect of grid size on the calculations, and an updated version of the original BEDMAP (ALBMAP: Le Brocq et al., 2010) was used as a data comparison. The formation of subglacial lakes influence ice dynamics and cause a flattening of the ice-surface slope. This opens up a potentially circular argument because the predictions will tend to pick up the resultant flat ice-surfaces rather than the initial hydraulic minima that caused the subglacial lake to form. To account for this circularity the ice-surfaces of BEDMAP2 and ALBMAP were smoothed to remove surface features, effectively removing any ice-surface elevation perturbations that reflect existing lakes. Deglacial ice and bed topographies at 5, 10, 15 and 20 thousand-year intervals were derived from the glimmer-community ice-sheet model; the margins and thicknesses are constrained by an extensive database of geological and glaciological information (see Whitehouse et al., 2012, for a full description of the model).

Cells that have more than 5000 cells flowing into them were used to arbitrarily define networks of meltwater flow concentration. A simulated subglacial lake was deemed successful in predicting a known subglacial lake if it was within a buffer defined by the known lake's length. Where the subglacial lake's length was not recorded or known we used the modal length (5 km), taken from the latest lake inventory (Wright and Siegert, 2011). Two statistics were calculated to investigate the ability of the predictions to replicate the known distribution of subglacial lakes:

- The percentage of known subglacial lakes identified by the predictions;
- the percentage of the predictions that correspond to a known subglacial lake location.

The sensitivity of the subglacial lake predictions was also investigated by:

- Arbitrary lowering the F-fraction to 0.75 to demonstrate an increase in the importance of the bed slope relative to ice-surface slope.
- Deriving subglacial lake predictions in regions of the bed where blocks of high density radio-echo sounding data have been collected (see Fretwell et al., 2013), so as to reduce the influence of gridding artefacts and smoothing on subglacial lake predictions.
- Calculating the percentage of known lakes ≥ 5 km long identified from the predictions and discarding those simulated lakes $< 5\,\mathrm{km}^2$ to explore the influence of subglacial lake size.
- Using a modelled basal thermal regime (from Pattyn, 2010, Fig. 1b) to mask out subglacial lakes predicted to form in cold-bedded regions of the bed where meltwater is absent.

TCD
7, 1177–1213, 2013

2.3 Greenland datasets

DEMs of ice-surface and bed topographies (from Bamber et al., 2001a,b) were used to calculate hydraulic potential surface at the bed of the Greenland Ice Sheet (GrIS) on a 5 km grid. To investigate subglacial hydrological changes of the GrIS since the Last Glacial Maximum (LGM, 21 thousand years ago), output from Huy2, a three-dimensional thermomechanical model (Simpson et al., 2009) was used to produce ice-surface and bed topographies at 1 thousand year time-slices through the evolution of the ice sheet for both $F = 1$ and $F = 0.75$. Importantly, the model is constrained by, and in good agreement with, observations of relative sea level as well as field data on past ice extent (Simpson et al., 2009). Likelihood maps indicating the percentage time that subglacial lakes existed throughout deglaciation thus far were derived, to explore the stability and evolution of the simulated subglacial lakes.

3 Simulating subglacial meltwater drainage and lakes under the Antarctic Ice Sheet

3.1 Present day Antarctic Ice Sheet

The subglacial drainage pattern produced for the BEDMAP2 dataset (grid size of 1 km) and for $F = 1$, is displayed in Fig. 1a, and provides an update of the work presented by Wright et al. (2008) using BEDMAP (grid size of 5 km). Meltwater flow is arranged in a series of discrete catchments, with meltwater flowing from central ice-divides towards the margin. Drainage networks reveal subtle variations in their geometry, including: (i) classical dendritic; (ii) angular; (iii) convergent; and (iv) parallel patterns (see inset circles in Fig. 1a). Subglacial meltwater tends to be concentrated along the major fast-flowing ice stream corridors where the ice-surface has been lowered relative to the surrounding ice sheet. Of the known subglacial lakes, the largest, Subglacial

TCD
7, 1177–1213, 2013

Lake Vostok (East Antarctica) is shown to drain through the Transantarctic Mountains (Fig. 1a).

Simulated subglacial lakes are relatively commonplace, with 31 250 simulated lakes, occurring over ~ 4 % of the grounded AIS (Fig. 1a, Table 1), dropping to 12 662 and 2.5 % respectively when cold-bedded regions are masked out (Fig. 1b, Table 1). They are prevalent beneath the East and West Antarctic ice sheets, occurring at a range of scales and congregating below ice-streams and ice-divides, often along or at the source of major subglacial drainage routeways. Rugged regions of the bed display a greater tendency towards ponding, as do localities where the ice-surface has a rough texture; the curvi-linear distribution of simulated subglacial lakes inland of the Transantarctic Mountains is primarily a result of surface irregularities. The most significant subglacial lakes are observed beneath ice-divides, with the largest located close to the South Pole and second-largest successfully delimiting Subglacial-Lake Vostok (Fig. 1a). In contrast, they are relatively rare beneath the rugged Antarctic Peninsula hinterland where they typically form small lakes.

Of the known subglacial lakes, 70 % are successfully predicted from the BEDMAP2 dataset, rising to 86 % when just those lakes ≥ 5 km long are considered (Table 1; Fig. 1a). Predictions restricted to the most densely-surveyed zones of the bed generate 4296 lakes and successfully identify 63 % of the known subglacial lakes and 94 % of the subglacial lakes ≥ 5 km long. In contrast, the smoothed, 5 km and 10 km re-gridded datasets, and ALBMAP grids are less capable of predicting known subglacial lakes (Table 1). However, there is little empirical difference between BEDMAP2 and ALBMAP predictions of the same resolution, and comparable results are also observed from the preferential selection of densely-surveyed bed regions (Table 1). For the BEDMAP2 dataset, those known subglacial lakes located within 100 km of an ice-divide have a 54 % success rate, compared to 75 % for those located further than 100 km away. In addition, where the ice is < 2500 m thick, 81 % of the known subglacial lakes are successfully identified, compared to 66 % beneath ice > 2500 m thick. This suggests the model is better at identifying known subglacial lakes in ice-stream regions than beneath ice-divides.

Given the high frequency of simulated subglacial lakes (Table 1) it is conceivable the high success rates could occur by chance. In other words, the large number of simulated lakes may preclude a low percentage of hits because they occupy a large expanse of the ice sheet bed. To test this we randomly redistribute the 386 known subglacial lakes and recalculate the percentage that are successfully predicted. Despite carrying out multiple iterations percentages between 30–35 % are consistently recorded. This gives us confidence that the high success rates are real and not an artefact of chance.

For the same scenarios, we also looked at the percentage of simulated subglacial lakes that correspond to known subglacial lake locations. This is more complicated because we do not have a complete inventory of subglacial lakes, and so a negative result does not preclude a correct prediction. Of the simulated subglacial lakes derived from BEDMAP2, only 3 % occur within the buffer zone of known subglacial lakes, with this value rising to 7 % when just those lakes $\geq 5\,km^2$ are included in the calculations (Table 1). Simulations restricted to densely-surveyed zones of the bed perform slightly better, with 5 % of the simulated lakes corresponding to known subglacial lake localities, and 12 % when just those simulated subglacial lakes $\geq 5\,km^2$ are included (Table 1). Similarly, when subglacial lakes in cold-bedded regions of the AIS are masked out the simulations record a 5 % success rate, rising to 9 % when simulated subglacial lakes $\geq 5\,km^2$ alone are considered.

3.2 Deglaciation of the Antarctic Ice Sheet since the LGM

Figure 2 reveals the simulated drainage patterns and subglacial lake predictions at 20, 15, 10 and 5 thousand year timeslices during the deglaciation of the AIS. These suggest that meltwater drainage under the AIS was relatively stable throughout deglaciation thus far, with drainage configurations comparable to the present-day ice sheet (see Fig. 1a). However, significant meltwater switches and drainage capture are observed.

For instance, meltwater flow from Subglacial Lake Vostok, which is currently predicted to drain through the Transantarctic Mountains (Fig. 1a), is simulated to drain towards Wilkes Land during the four deglacial time-slices (Fig. 2). Furthermore, the Siple Coast drainage network repeatedly shifted position as ice retreated (see Fig. 3). Indeed, during the 15 000 yr time-slice meltwater was captured and focused through a single (dominant) pass in the Transantarctic Mountains, while at 20 and 10 thousand-years before present two major drainage routeways were thought to have been in operation (Fig. 3). By 10 000 yr ago, the western-most drainage network (basin 1 in Fig. 3) had been almost completely subsumed by its neighbouring catchment, and by 5000 yr before present West Antarctica was providing the majority of the meltwater instead of East Antarctica, which previously dominated.

Simulated subglacial lakes are relatively stable during deglaciation, especially beneath ice-divides in East Antarctica. However, short-lived subglacial lake formation is predicted during expansion of ice to the shelf edge throughout the Antarctic Peninsula, parts of West Antarctica, across the continental shelf and through the Transantarctic Mountains (Fig. 2). The frequency distribution of simulated subglacial lake areas is similar for all four deglacial timeslices and a similar pattern if also observed for the present-day ice-sheet configuration (Fig. 4). Although very large subglacial lakes, greater than 300 km^2, are simulated, the vast majority are < 5 km^2 in size. This pattern is comparable to the distribution of known subglacial lake lengths, although the slight drop in frequency observed in the smallest (< 12 km long) known lakes is not replicated by the simulations (Wright and Siegert, 2011).

4 Simulating subglacial meltwater drainage and lakes under the Greenland Ice Sheet

Whereas subglacial lakes are commonly observed and predicted beneath the AIS (e.g. Wright and Siegert, 2011), there is no evidence for subglacial lakes existing beneath the GrIS. This seems incongruous given observations detailing the widespread

TCD
7, 1177–1213, 2013

presence of subglacial meltwater at its bed (Dahl-Jenson et al., 2003; Oswald and Gogineni, 2008, 2012). Is this because there are no subglacial lakes? If so, what conditions inhibit their formation? Or are there subglacial lakes at the bed that remain to be found?

Given the high percentage of known subglacial lakes predicted beneath the AIS (Sect. 3) we suggest simple hydrological calculations can be a useful tool for simulating subglacial lakes and drainage pathways beneath other (palaeo-)ice sheets. With this in mind, we now investigate the subglacial drainage network of the GrIS in its present and past states, including the potential for subglacial lake formation.

4.1 Present-day Greenland Ice Sheet

Subglacial lakes and meltwater drainage networks are displayed in Fig. 5, where they are compared against ice-surface velocity measurements (Joughin et al., 2010) and observed hydrological outlets at the ice-sheet margin (after Lewis and Smith, 2009).

Like Antarctica, meltwater drainage beneath the GrIS is organised into a series of discrete catchments composed of dendritic pathways that broadly flow from the ice-sheet centre to the margin (Fig. 5). Meltwater flow concentration is demonstrated along the fast-flowing corridors of the ice sheet, with significant drainage networks feeding the Northeast Greenland Ice Stream (NEGIS) (108 925 km^2), Jakboshavn Isbrae (103 575 km^2) and the Petermann Glacier (61 850 km^2) (Fig. 5b). A qualitative relationship is also observed between ice-surface velocity and the size of the meltwater drainage network. Moreover, a good general agreement between predicted and known meltwater outlets was demonstrated by Lewis and Smith (2009) (Fig. 5a).

The hydrological modelling simulates ninety subglacial lakes beneath the GrIS, which cover $\sim 0.2\,\%$ of the GrIS bed. They are typically small features located in the rugged eastern sector of the ice sheet, close to ice divides. Indeed, apart from the Petermann Glacier and NEGIS there is little evidence for ponding beneath the fast-flowing arteries of the ice sheet (Fig. 5b). Moreover, there is a paucity of subglacial lakes within the deep basin of the northern sector of the ice sheet, where the main north-south ice-divide is situated (Fig. 5). However, despite the 5 km grid size and low frequency a similar distribution of subglacial lake areas to the AIS is observed (Fig. 4).

4.2 Deglaciation of Greenland Ice Sheet since the Last Glacial Maximum

Like Antarctica, meltwater drainage under the GrIS is predicted to have been broadly stable, with little large-scale re-organisation in hydrology since the LGM (Fig. 6). However, subtle switches in subglacial water drainage are still demonstrated (Fig. 6). For instance, in west Greenland the northern limb of the Jakobshavn drainage network was captured by the Uummannaq system 16 000 yr ago; and the NEGIS drainage catchment expanded southwards during the 10 000 yr timeslice (Fig. 6). Also, between 12 and 11 thousand years the north GrIS, which was previously (and subsequently) dominated by NW and NE subglacial drainage pathways become a key hydrological connection to the western sector of the ice sheet (Fig. 6).

Subglacial lakes are predicted at all time-slices through the evolution of the GrIS (Figs. 6, 7, 8). More than 300 subglacial lakes are simulated at each of the time-slices between 19 and 16 thousand years ago, with the number then dropping rapidly to < 70 lakes by 9000 yr before present whereupon it remained relatively steady. Likelihood predictions for $F = 1$ show a tendency for subglacial lake formation in mountainous terrain, both along the eastern sector of the ice sheet and within fjords (Fig. 7a). Between 19 and 11 thousand years ago > 40 % of the predicted lakes are located beyond the present ice-margin position. Lakes are typically small and do not show much proclivity for stability throughout the evolution of the ice sheet. In contrast, subglacial lake formation is extensive for $F = 0.75$, and the lakes are large, remaining relatively stable throughout deglaciation (7b).

Figure 8a demonstrates a decrease in the area covered by subglacial lakes concomitant with a reduction in GrIS size. The period of greatest ice recession, between 14 and 10 thousand years ago, is associated with the largest reduction in subglacial lakes (Fig. 8a). However, the change in subglacial lake area does not decline linearly with ice sheet size. This is illustrated by the decline in percentage of the grounded ice-sheet bed occupied by subglacial lakes as the ice-sheet waned (Fig. 8b). Similarly a rough decline is observed for the four modelled Antarctic deglacial timeslices.

5 Interpretation and discussion

5.1 Antarctica

5.1.1 Known subglacial lakes predicted

Results presented in Sect. 3.1 demonstrate hydraulic potential calculations are able to successfully predict a large percentage of known subglacial lakes (> 70 %) beneath the AIS. The incorporation of the subglacial lake-surface reflector in the bed topography and thickness grids has generally been considered a fatal flaw in using hydrological potential equations to identify subglacial lake locations. Yet, the high percentage of subglacial lakes that are successfully predicted questions this logic. For instance, we are able to accurately delimit the extent of Subglacial-Lake Vostok (Fig. 1a) despite the incorporation of its lake-surface reflector into the BEDMAP2 topography grid. We suggest two reasons why this might be the case. Firstly, a subglacial lake would have to be filled to its hydraulic potential lip to fully smooth out the minima. While this might be the case for a few subglacial lakes that are just about to drain, the majority are likely to be at some intermediate state of filling (e.g. Smith, 2009, and references therein). Consequently, the hydraulic potential difference between the simulated lake lip and potential surface could be combined with recharge rates to estimate the time period leading up to drainage. Secondly, because of the coarse resolution of the grid (1 km or greater) lake outlets may become smoothed, therefore artificially raising the depth required to trigger drainage. Raising the base-level at which drainage may occur by smoothing the topography would, however, also pick-out basins not able to host subglacial lakes, leading to over-predictions (see Sect. 5.1.2).

TCD
7, 1177–1213, 2013

5.1.2 Simulations that predict a known subglacial lake

A large percentage of simulated subglacial lakes do not correspond to known subglacial lake locations (< 10 %). This could be due to: (i) error in the input datasets; (ii) because many of the subglacial lakes are yet to be identified; and/or (iii) processes not included in our simple model, e.g. dynamic spatial and temporal variations in water pressure. Of these options, the third is least preferable as it would indicate the model is not an appropriate technique for identifying or predicting subglacial lakes.

Despite our improved knowledge of the topography beneath the AIS, the number of 5 km cells containing radar data still only comprises 36 % of the grounded bed in the updated BEDMAP2 dataset (c.f., Fretwell et al., 2013). The percentage of the bed covered by radar surveys will be even lower as the data are lines (e.g. flight lines) not grids. A large part of the discrepancy between number of simulated and known subglacial lakes is therefore probably because of an incomplete knowledge of the bed, and in particular because of erroneous subglacial lakes associated with gridding artefacts (Fig. 1). Moreover, because we assume the bed is pervasively warm-bedded, subglacial lakes are predicted in regions that are currently cold-bedded with the potential for subglacial lake genesis. This will also result in numerous negative results (see Table 1, Fig. 1b). This inference is supported by the improved success of the simulations at predicting known subglacial lakes in densely-surveyed blocks of data and where cold-bedded regions are masked out (Table 1). Although our simulations show the potential for subglacial lake genesis, and the frequency histograms (Fig. 4) hint at many small subglacial lakes yet to be found, discriminating between the two remaining error terms would require further validation of the results against radar data.

5.1.3 Subglacial lake predictions during the deglaciation of the Antarctic Ice Sheet

Increased subglacial lake genesis is predicted to have occurred when the ice sheet was larger and extended onto the continental shelf (Fig. 2). This includes repeated

TCD
7, 1177–1213, 2013

palaeo-subglacial lake formation in the rugged interior of Marguerite Bay in isolated basins connected by meltwater channels (e.g. Anderson and Oakes-Fretwell, 2008), and the temporary formation of a shallow subglacial lake in Palmer Deep 15 thousand years ago (see Domack et al., 2006).

The ice-surface flattening feedback resulting from subglacial lake formation (e.g. Livingstone et al., 2012, and references therein) sets up the intriguing possibility that many of the present-day subglacial lakes have been inherited from past ice-sheet configurations, and would have already drained without this stabilizing feedback. Such an example of hysteresis implies that, for the same geometry, a retreating ice-sheet yields considerably more subglacial lakes' than one advancing. It therefore follows that many subglacial lakes formed during the last deglaciation, under different ice-sheet geometries, still exist beneath the present-day AIS. Table 2 gives some support for this, with 40–44 % of the known subglacial lakes successfully predicted during each deglacial timeslices, rising to 53 % when they are all included. Smoothing the ice-surface should remove inherited subglacial lakes whose existence depends on the ice-surface flattening feedback. Indeed, there is 15 % less chance of hitting a known subglacial lake when the BEDMAP2 ice-surface has been smoothed (Table 1). We can test whether the subglacial lakes, which have been smoothed out, were derived from past ice-sheet configurations by summing the smoothed subglacial lake simulations with those from the deglacial timeslices (see Table 2). The result is a 20 % increase in the ability to predict known subglacial lakes (to 75 %), which is twice that accomplished by summing the 1st order simulations with the deglacial timeslices (Table 2). This implies that the deglacial simulations can account for ∼ 20 % of the known subglacial lakes and that 10 % of subglacial lakes persist solely due to the ice-surface flattening feedback.

The implications of this stabilizing feedback on short-term subglacial lake stability and longer-term differences between advancing and retreating ice-sheet modes are unknown. Certainly, this work suggests that subglacial lakes are more pervasive (and therefore of greater importance) during the deglacial phase, which has resonance for ice-stream formation and flow, bed lubrication, meltwater drainage and eventually ice-sheet collapse.

5.1.4 Meltwater drainage routeways

The meltwater drainage routeways simulated using BEDMAP2 result in a broadly similar network to that calculated by Wright et al. (2008). Subtle variations in the simulated drainage pattern beneath Antarctica (Fig. 1a) are thought to reflect broad underlying controls, such as slope and structure (c.f., Twidale, 2004, and references therein), on glacial processes. Classical dendritic patterns are typically associated with very slight surface slopes and/or regions with no significant structural control. It is therefore no surprise that this pattern characterises many of the interior zones of East Antarctica where ice-surface slopes were very low, and regions of the bed smoothed due to lack of data (Fig. 1a). In West Antarctica, especially inland of the Amundsen Sea, and south of the Transantarctic Mountains the patterns is more angular, perhaps due to strong structural/tectonic control (e.g. arrangement and spacing of fault and joints). The strongly convergent pattern of meltwater drainage, from the South Pole into the Ronne Ice Shelf, could reflect the former breaching of a large bedrock ridge, with the subsequent lowering of the drainage level leading to capture of the surrounding hydrology. Finally, strongly parallel drainage geometries imply control of flow by gradient, which is in agreement with the ice-marginal drainage pattern where ice-surface slopes are greatest (Fig. 1a).

Figure 1b illustrates how various subglacial drainage routeways, especially around coastal sectors of the EAIS (e.g. Dronning Maud Land, Terra Adélie and Enderby Land) traverse cold-bedded zones not conducive to meltwater generation or drainage (see Pattyn, 2010). These cold-bedded rims may in some cases act as natural seals, promoting subglacial meltwater storage up ice-flow, and/or diverting drainage pathways (see Livingstone et al., 2012).

Wright et al. (2008) demonstrate that hydrological flow directions can be highly sensitive to slight changes in ice-surface topography. And although the broad-scale pattern of meltwater flow during the last deglaciation is predicted to have been broadly stable (Fig. 2), we also note several regions susceptible to drainage capture or migration. For instance, we observe a similar sensitivity in the drainage of Subglacial Lake Vostok (c.f., Wright et al., 2008). Moreover, the Siple Coast drainage configuration is shown to have shifted repeatedly during deglaciation (Fig. 3). This is probably due to the low angle of ice slope, which leaves the neighbouring ice stream drainage networks vulnerable to minor changes in ice thickness. It is perhaps no surprise then that ice-stream stagnation interpreted to indicate meltwater capture has been observed between two of the contemporary ice streams in this region (Anandakrishnan and Alley, 1997; Vaughan et al., 2008). Our analysis suggests this may have been a common occurrence during the last deglaciation, with implications for ice stream behaviour.

5.2 Greenland

5.2.1 Subglacial lakes beneath the present-day Greenland Ice Sheet

In contrast to the AIS, the scarcity of subglacial lakes simulated beneath the present-day GrIS (~ 0.2 % of bed area) suggests they are not a major component of the hydrological network. Indeed, this result is probably an overestimate because the bed is not wholly warm-based. Geophysical radar data from North Greenland suggest that only 13–20 % of the bed is thawed (Oswald and Gogineni, 2008, 2012), while there is little evidence for subglacial lakes beneath warm-based ice stream corridors (Fig. 5b). That this simplified analysis of the subglacial hydrology is not able to produce widespread ponding of subglacial meltwater leads us to deduce that the bed and ice-surface geometry of the GrIS is not conducive to significant subglacial lake development. Since the influence of the ice-surface on hydraulic potential is about ten times that of the bed (e.g. Shreve, 1972) the lack of subglacial lakes can be reconciled with the steep ice-surface gradients of the GrIS compared to the AIS (see Fig. 9). However, not all water is able to escape, and where the bed is rough, such as in the mountainous eastern sector of the ice sheet, subglacial lake formation ($\geq 5\,km^2$) is possible (Fig. 7). Indeed, it can be

TCD
7, 1177–1213, 2013

speculated that with higher resolution bed topographies many more smaller subglacial lakes below the resolution of the grid would be predicted in the rugged mountainous hinterlands. This view is supported by the frequency histogram distributions (Fig. 4) and data for Antarctica (Table 1), which reveals the large number of lake simulations below 5 km, and the improved success rate with higher resolutions respectively. The analysis therefore implies that whilst no subglacial lakes have been found beneath the GrIS to date, the ice- and bed-topographies do permit limited lake formation, although with a different distribution, size and depth to those beneath Antarctica (see also Livingstone et al., 2012). We therefore predict that it is a matter of time before subglacial lakes are also identified beneath Greenland and that our lake prediction locations (both present day and during deglaciation) may provide useful targets for geophysical studies to discover lakes.

5.2.2 Subglacial lake evolution during the deglaciation of the Greenland Ice Sheet

The abundance of subglacial lakes is simulated to decline as the GrIS waned, and as the ice-sheet shrank so too did the propensity for subglacial lake genesis (Fig. 8). This is attributed to changes in the ice-surface slope (Fig. 9); subglacial lake formation is favoured when a greater proportion of the ice sheet is flat and when the mountainous rim no longer coincides with the steep ice-sheet margin. In addition, Fig. 8b demonstrates how the percentage of the ice-sheet bed occupied by subglacial lakes changed more rapidly (i.e. the gradient was steeper) during the initial stages of deglaciation (19–10 thousand years ago) when the ice-sheet was larger (Fig. 8b). This implies that subglacial lakes are more sensitive to changes in ice-sheet size when the ice sheet is larger (i.e. for a given change in ice-sheet area the change in subglacial lake extent is of a higher magnitude).

When the GrIS had expanded onto the continental shelf (19–11 thousand years ago) $> 40\,\%$ of the simulated subglacial lakes lay outside of the present-day ice-margin, and would therefore have emerged from under the ice. Other lakes formed within the bounds of the present-day ice-sheet, but predicted to have drained (Fig. 8) may have survived deglaciation due to the ice-surface flattening feedback (see Sect. 5.1.3).

5.2.3 Meltwater drainage routeways

The dendritic pattern of subglacial meltwater flow-pathways simulated in this study (Fig. 5) is consistent with the results of Lewis and Smith (2009), and also broadly similar in form to that simulated beneath the AIS. The simulated evolution of the subglacial drainage network since the LGM (Fig. 6) demonstrates the susceptibility of some localities of the ice sheet to subglacial drainage switches, driven by subtle changes in ice-surface and bed geometry. Significantly, some of the major present-day ice streams, such as NEGIS and Jakobshavn, display significant changes to their subglacial water flowpaths over time (Fig. 6). As for Antarctica, we predict drainage shifts could play a crucial role in controlling ice-streaming and behaviour.

6 Conclusions

6.1 Subglacial lakes

– The Shreve hydraulic potential equation and simple routing mechanisms in a GIS can be used to successfully identify a high percentage ($>70\,\%$) of the known subglacial lakes beneath the AIS. Significantly, we demonstrate how known subglacial lakes are predicted despite their surface-level being used to calculate the bed-topography and ice thicknesses used in the calculations. We reason this is because: (i) most lakes are not completely full (i.e. at intermediate states of filling); and (ii) the grid-resolution smooth's out the base-level at which drainage may occur. In particular, the larger subglacial lakes are easiest to predict, although these make up only a small percentage of the overall distribution of lake sizes.

TCD
7, 1177–1213, 2013

- The simulations produce significantly more subglacial lakes than those presently identified beneath the AIS. Thus, a large percentage of simulated subglacial lakes do not correspond to known subglacial lake locations. Such a discrepancy is thought to primarily stem from an incomplete knowledge of the bed. And although we simplify the hydrological system, which will certainly result in an additional error term, we also suggest that hundreds if not thousands of subglacial lakes, particularly smaller ones, are yet to be found. These lake predictions might therefore form useful targets for future radar surveys.
- By applying the same method to the GrIS we demonstrate the potential for subglacial lake formation at its bed. However, in contrast to Antarctica the subglacial lakes are shown to occupy a smaller fraction of the grounded ice-sheet bed and are characteristically small features. Their relative rarity is a result of steep surface gradients (Figs. 8 and 9).
- We illustrate how the subglacial lake – ice-surface flattening feedback means many present-day subglacial lakes have been inherited from past ice-sheet configurations, and would have already drained without this stabilizing effect. Moreover, the resultant hysteresis, whereby a retreating ice-sheet will have many more subglacial lakes than one advancing, has implications for ice-stream formation and flow, bed lubrication and meltwater drainage.

6.2 Drainage pathways

- Modelling the present-day drainage networks beneath the Antarctic and Greenland ice sheets have elucidated major meltwater routeways and the form they take. In Antarctica dendritic, angular, convergent and parallel drainage routeways have all been simulated, which have been related to underlying (ice and bed) slope and structural controls.

TCD
7, 1177–1213, 2013

- The evolution of the Greenland and Antarctic subglacial drainage networks were assessed by simulating basal meltwater flow at discrete time intervals over the last 21 000 yr. We reveal key sectors of the two ice sheets that have been vulnerable to past drainage switches. In particular, neighbouring ice-stream drainage networks (e.g. the Siple Coast sector, AIS and the NEGIS, Greenland) with their low-angled slopes are shown to be particularly sensitive to small changes in ice-geometry.

6.3 Further applications

- The predictability of subglacial lakes beneath the AIS using hydraulic potential equations and routing techniques suggests this is also a viable methodology for predicting palaeo-subglacial lakes beneath the great Quaternary Northern Hemisphere Ice Sheets (see Evatt et al., 2006; Livingstone et al., 2013). This approach has the benefit of comprehensive information on the bed properties, but relies on modelled ice-surface topographies.

Acknowledgements. This work was supported by a NERC Early Career Research Fellowship awarded to SJL (NE/H015256/1). We thank Matt Simpson, Pippa Whitehouse and Frank Pattyn for supplying ice-sheet model output on the deglaciation of the Greenland Ice Sheet and Antarctica Ice Sheet, and modelled basal temperature data respectively.

References

Anandakrishnan, S. and Alley, R. B.: Stagnation of Ice Stream C, West Antarctica by water piracy, Geophys. Res. Lett., 24, 265–268, 1997. 1194

Anderson, J. B. and Oakes-Fretwell, L.: Geomorphology of the onset area of a palaeo-ice stream, Marguerite Bay, Antarctic Peninsula, Earth Surf. Proc. Land., 33, 503–512, 2008. 1192

Bamber J. L., Layberry, R. L., and Gogineni, S. P.: A new ice thickness and bed data set for the Greenland Ice Sheet: 1. Measurement, data reduction, and errors, J. Geophys. Res., 106, 33773–33780, 2001a. 1184

TCD
7, 1177–1213, 2013

Bamber J. L., Layberry, R. L., and Gogineni, S. P.: A new ice thickness and bed data set for the Greenland Ice Sheet: 2. Relationship between dynamics and basal topography, J. Geophys. Res., 106, 33781–33788, 2001b. 1184

Bartholomew, I., Nienow, P., Mair, D., Hubbard, A., King, M. A., and Sole, A.: Seasonal evolution of subglacial drainage and acceleration in a Greenland outlet glacier, Nat. Geosci., 3, 408–411, doi:10.1038/ngeo863, 2010. 1179

Clarke, G. K. C.: Subglacial processes, Ann. Rev. Earth Planet. Sci., 33, 247–276, 2005. 1179, 1181

Cuffey, K. M. and Patterson, W. S. B.: The Physics of Glaciers, 4th edn., Elsevier, 2010.

Dahl-Jensen, D., Gundestrup, N., Gogineni, S. P., and Miller, H.: Basal melt at NorthGRIP modelled from borehole, ice-core and radio-echo sounder observations, 37, 207–212, 2003. 1188

Domack, E., Amblás, D., Gilbert, R., Brachfield, S., camerlenghi, A., Rebesco, M., Canals, M., and Uregeles, R.: Subglacial morphology and glacial evolution of the Palmer deep outlet system, Antarctic Peninsula, Geomorphology, 75, 125–142, 2006. 1192

Evatt, G. W., Fowler, A. C., Clark, C. D., and Hulton, N. R. J.: Subglacial floods beneath ice sheets, Philos. T. Roy. Soc. A, 374, 1769–1794, 2006. 1180, 1182, 1198

Fretwell, P., Pritchard, H. D., Vaughan, D. G., Bamber, J. L., Barrand, N. E., Bell, R., Bianchi, C., Bingham, R. G., Blankenship, D. D., Casassa, G., Catania, G., Callens, D., Conway, H., Cook, A. J., Corr, H. F. J., Damaske, D., Damm, V., Ferraccioli, F., Forsberg, R., Fujita, S., Gim, Y., Gogineni, P., Griggs, J. A., Hindmarsh, R. C. A., Holmlund, P., Holt, J. W., Jacobel, R. W., Jenkins, A., Jokat, W., Jordan, T., King, E. C., Kohler, J., Krabill, W., Riger-Kusk, M., Langley, K. A., Leitchenkov, G., Leuschen, C., Luyendyk, B. P., Matsuoka, K., Mouginot, J., Nitsche, F. O., Nogi, Y., Nost, O. A., Popov, S. V., Rignot, E., Rippin, D. M., Rivera, A., Roberts, J., Ross, N., Siegert, M. J., Smith, A. M., Steinhage, D., Studinger, M., Sun, B., Tinto, B. K., Welch, B. C., Wilson, D., Young, D. A., Xiangbin, C., and Zirizzotti, A.: Bedmap2: improved ice bed, surface and thickness datasets for Antarctica, The Cryosphere, 7, 375–393, doi:10.5194/tc-7-375-2013, 2013. 1182, 1183, 1191

Fricker, H. A., Scambos, T., Bindschadler, R., and Padman, L.: An active subglacial water system in West Antarctica mapped from space, Science, 315, 1544–1548, 2007. 1179

Hallet, B.: Subglacial regelation water film, J. Glaciol., 17, 209–221, 1979. 1179

Hubbard, B., Sharp, M. J., Willis, I. C., Neilsen, M. K., and Smart, C. C.: Borehole water-level variations and the structure of the subglacial hydrological system of Haut Glacier d'Arolla, Valais, Switzerland, J. Glaciol., 41, 572–583, 1995. 1179

Joughin, I., Smith, B. E., Howat, I. M., Scambos, T., and Moon, T.: Greenland flow variability from ice-sheet wide velocity mapping, J. Glaciol., 56, 415–430, 2010. 1188, 1209

Kamb, B.: Glacier surge mechanism based on linked cavity configuration of the basal water conduit system, J. Geophys. Res., 96, 585–595, 1987. 1179

Kamb, B.: Basal zone of the West Antarctic ice streams and its role in lubrication of their rapid motion, in: The West Antarctic Ice Sheet: behaviour and environment, edited by: Alley, R. B. and Bindschadler, R. A., Antarctic Research Series, 77, Washington DC, American Geophysical Union, 157–199, 2001. 1181

Lappegard, G., Kohler, J., Jackson, M., and Hagen, J. O.: Characteristics of subglacial drainage systems deduced from load-cell measurements, J. Glaciol., 52, 137–148, 2006. 1179

Le Brocq, A. M., Payne, A. J., and Vieli, A.: An improved Antarctic dataset for high resolution numerical ice sheet models (ALBMAP v1), Earth Syst. Sci. Data, 2, 247–260, doi:10.5194/essd-2-247-2010, 2010. 1182

Lewis, S. M. and Smith, L. C.: Hydrological drainage of the Greenland Ice Sheet, Hydrol. Process., 23, 2004–2011, 2009. 1188, 1196, 1209

Livingstone, S. J., Clark, C. D., Piotrowski, J. A., Tranter, M. J., Bentley, M. J. Hodson, A., Swift, D. A., and Woodward, J.: Theoretical framework and diagnostic criteria for the identification of palaeo-subglacial lakes, Quaternary Sci. Rev., 55, 88–110, 2012. 1180, 1192, 1193, 1195

Livingstone, S. J., Clark, C. D., and Tarasov, L.: North American palaeo-subglacial lakes and their meltwater drainage pathways: predictions and geomorphological clues to their origin, Earth Planet. Sci. Lett., in review, 2013. 1198

Lliboutry, L.: Local friction laws for glaciers: a critical review and new openings, J. Glaciol., 23, 67–95, 1979. 1179

Nienow, P. W., Sharp, M., and Willis, I.: Seasonal changes in the morphology of the subglacial drainage system, Haut Glacier d'Arolla, Switzerland, Earth Surf. Proc. Land., 23, 825–843, 1998. 1179

Oswald, G. K. A. and Gogineni, S. P.: Recovery of subglacial water extent from Greenland radar survey data, J. Glaciol., 54, 94–106, 2008. 1188, 1194

Oswald, G. K. A. and Gogineni, S. P.: Mapping basal melt under the Northern Greenland Ice Sheet, IEEE T. Geosci. Remote, 50, 585–592, 2012. 1188, 1194

Pattyn, F.: Antarctic subglacial conditions inferred from a hybrid ice sheet/ice stream model, Earth Planet. Sci. Lett., 295, 451–561, 2010. 1179, 1183, 1193, 1203, 1205

Robin, G. de Q., Swithinbank, C. W. M., and Smith, B. M. E.: Radio Echo Exploration of the Antarctic Ice Sheet, International symposium on Antarctic glaciological exploration (ISAGE), Hannover, New Hampshire, USA, 3–7 September 1968, 1970. 1179

Röthlisberger, H.: Water pressure in intra- and subglacial channels, J. Glaciol., 11, 177–203, 1972. 1179

Schoof, C.: Ice-sheet acceleration driven by melt supply variability, Nature, 468, 803–806, 2010. 1179

Sharp, M., Gemmell, J. C., Tison, J.-L.: Structure and stability of the former subglacial drainage system of the Glacier de Tsanfleuron, Switzerland, Earth Surf, Proc. Land., 14, 119–134, 1989. 1179

Shreve, R. L.: Movement of water in glaciers, J. Glaciol., 11, 205–214, 1972. 1180, 1181

Siegert, M. J., Le Brocq, A., and Payne, A. J.: Hydrological connections between Antarctic subglacial lakes, the flow of water beneath the East Antarctic Ice Sheet and implications for sedimentary processes, in: Glacial Sedimentary Processes and Products, edited by: Hambrey, M. J., Christoffersen, P., Glasser, N. F., and Hubbard, B., Special Publication 39 of the IAS, Wiley-Blackwell, 2007. 1180, 1182

Simpson, M. J. R., Milne, G. A., Huybrechts, P., and Long, A. J.: Calibrating a glaciological model of the Greenland Ice Sheet from the Last Glacial Maximum to present-day using field observations of relative sea level and ice extent, Quaternary Sci. Rev., 28, 1631–1657, 2009. 1184, 1210

Smith, B. E., Fricker, H. A., Joughin, I. R., and Tulaczyk, S.: An inventory of active subglacial lakes in Antarctica detected by ICESat (2003–2008), J. Glaciol., 55, 573–595, 2009. 1179, 1190

Twidale, C. R.: River patterns and their meaning, Earth Sci. Rev., 67, 159–218, 2004. 1193, 1205

Vaughan, D., Corr, H. F. J., Smith, A. M., Pritchard, H., and Shephard, A.: Flow-switching and water piracy between Rutford Ice Stream and Carlson Inlet, West Antarctica, J. Glaciol., 54, 41–48, 2008. 1194

Walder, J. S. and Hallet, B.: Geometry of former subglacial water channels and cavities, J. Glaciol., 23, 335–346, 1979. 1179

Whitehouse, P. L., Bentley, M. J., and Le Brocq, A. M.: A deglacial model for Antarctica: geological constraints and glaciological modelling as a basis for a new model of Antarctic glacial isostatic adjustment, Quaternary Sci. Rev., 32, 1–24, 2012. 1183, 1206, 1207

Wingham, D. J., Siegert, M. J., Shepherd, A., and Muir, S.: Rapid discharge connects Antarctic subglacial lakes, Nature, 440, 1033–1036. 1179

Wright A. P. and Siegert M. J.: The identification and physiographical setting of Antarctic subglacial lakes: an update based on recent advances, in: Subglacial Antarctic Aquatic Environments, edited by: Siegert, M. J., Kennicutt, C., and Bindschadler, B., AGU Monograph, 2011. 1179, 1180, 1183, 1187, 1203

Wright, A. P., Siegert, M. J., Le Brocq, A. M., and Gore, D. B.: High sensitivity of subglacial hydrological pathways in Antarctica to small ice-sheet changes, Geophys. Res. Lett., 45, L17504, doi:10.1029/2008GL034937, 2008. 1180, 1182, 1184, 1193, 1194

Table 1. Predicted AIS subglacial lake statistics.

Subglacial lake predictions		BEDMAP2 (1 km)	BEDMAP2 (F = 0.75)	BEDMAP2 (1 km, smoothed)	BEDMAP2 (5 km)	BEDMAP2 (10 km)	ALBMAP (5 km)	ALBMAP (5 km, smoothed)
Number of predicted subglacial lakes	1st order prediction	31250	22898	7328	1581	984	1629	418
	Warm-bedded[c]	12662	8665	3191	719	611	1089	260
	Densely-surveyed blocks[b]	4296	–	1620	373	183	–	–
Percentage of known lakes[a] predicted	1st order prediction	70.47	77.72	54.92	28.76	24.35	31.09	14.51
	Known lakes ≥ 5 km	85.59	94.07	74.58	52.54	42.37	47.46	32.2
	Warm-bedded[c]	70.75	77.87	58.1	31.62	28.85	36.36	18.18
	Warm-bedded and with known lakes ≥ 5 km	87.64	93.26	78.65	58.43	55.06	57.3	35.96
	Densely-surveyed blocks[b]	63	–	52.5	30	25	–	–
	Densely-surveyed blocks with known lakes ≥ 5 km	94.34	–	84.91	64.15	50.94	–	–
Percentage of simulations that predict a known lake	1st order prediction	2.88	1.97	4.57	7.91	10.87	8.9	11.24
	Simulated subglacial lakes ≥ 5 km^2	6.84	3.71	8.58	N/A	N/A	N/A	N/A
	Warm-bedded[c]	4.82	3.14	7.3	13.21	14.07	9.64	15.38
	Warm-bedded and simulated subglacial lakes ≥ 5 km^2	8.6	5.33	11.03	N/A	N/A	N/A	N/A
	Densely-surveyed blocks[b]	4.7	–	6.6	11.8	18.6	–	–
	Densely-surveyed blocks and simulated subglacial lakes ≥ 5 km^2	11.47	–	15.56	N/A	N/A	–	–

[a] known lakes derived from Wright and Siegert (2011);
[b] Densely-surveyed blocks of radio-echo sounding data, where gridding artefacts are less prevalent (F = 0.75 and ALBMAP not included in these calculations);
[c] Warm-bedded refers to the inclusion of modelled basal temperate Pattyn (2010).

TCD
7, 1177–1213, 2013

Table 2. Ice surface flattening feedback and subglacial lake inheritance: the second to fifth rows illustrate the percentage of known subglacial lakes predicted by each of the modelled deglacial timeslices (20, 15, 10 and 5 thousand year intervals). The sixth row is the percentage of known subglacial lakes predicted by the summed deglacial timeslices, and the final two rows combine the summed deglacial timeslices with the 1st order and smoothed BEDMAP2 simulations. See text for detailed explanation.

Data	Percentage of discovered present-day subglacial lakes predicted
Present day (from Table 1)	70.47
5000 yr ago	39.64
10 000 yr ago	41.45
15 000 yr ago	40.93
20 000 yr ago	44.04
All deglacial intervals	53.12
BEDMAP2 and all deglacial time intervals	79.79
BEDMAP2 (smoothed) and all deglacial time intervals	74.61

TCD
7, 1177–1213, 2013

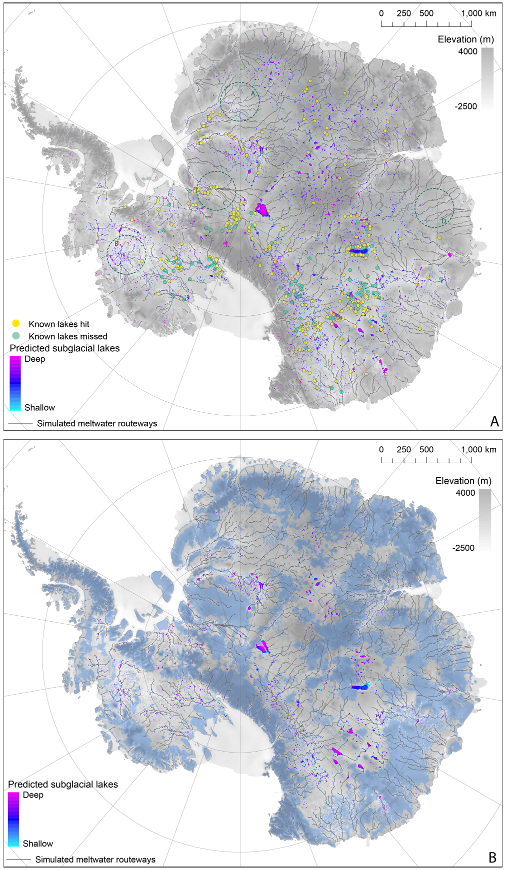

Fig. 1. Simulated subglacial drainage pathways and subglacial lakes beneath the AIS. **(A)** No basal thermal regime; **(B)** basal thermal regime (from Pattyn, 2010). In **(A)**, the four dark-green dotted circles illustrate the different types of drainage pattern (after Twidale, 2004) that characterise the bed of Antarctica (A: classical dendritic; B: angulate; C: convergent; and D: parallel). In **(B)**, the blue colour illustrates regions below the pressure melting point. This is used as a simple mask to remove all subglacial lakes that fall within the cold-bedded zones. Note, the subglacial drainage network is still treated as though the bed was wholly warm based.

TCD
7, 1177–1213, 2013

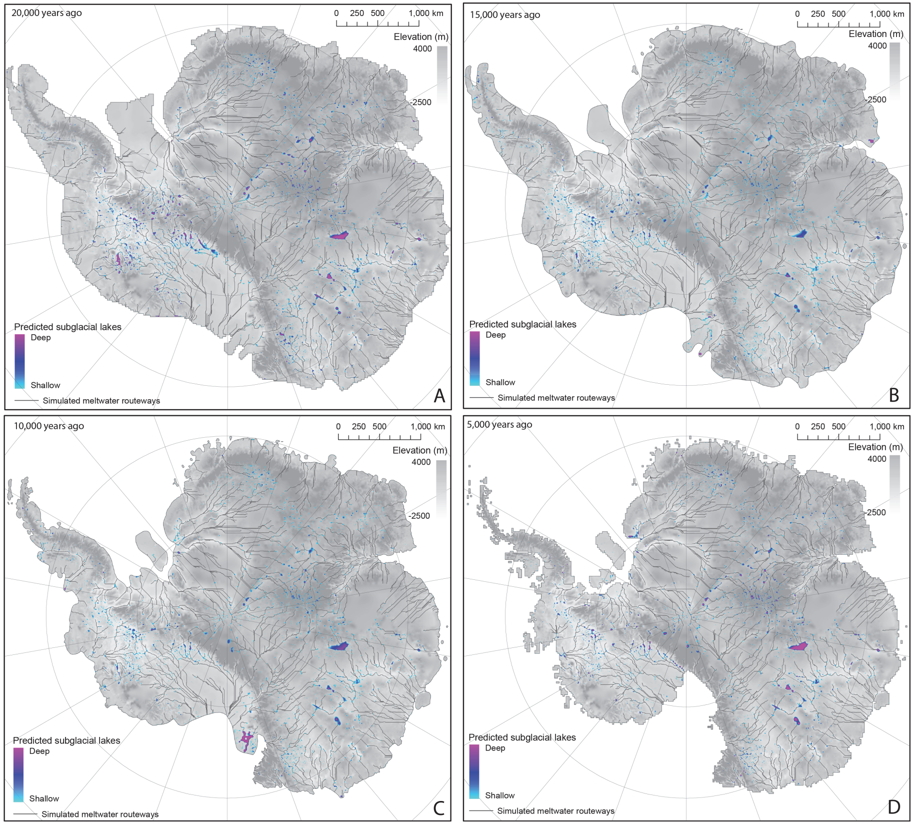

Fig. 2. Simulated subglacial drainage pathways and subglacial lakes at 5, 10, 15 and 20 thousand-year timeslices during the deglaciation of the AIS. The model used is from Whitehouse et al., 2012.

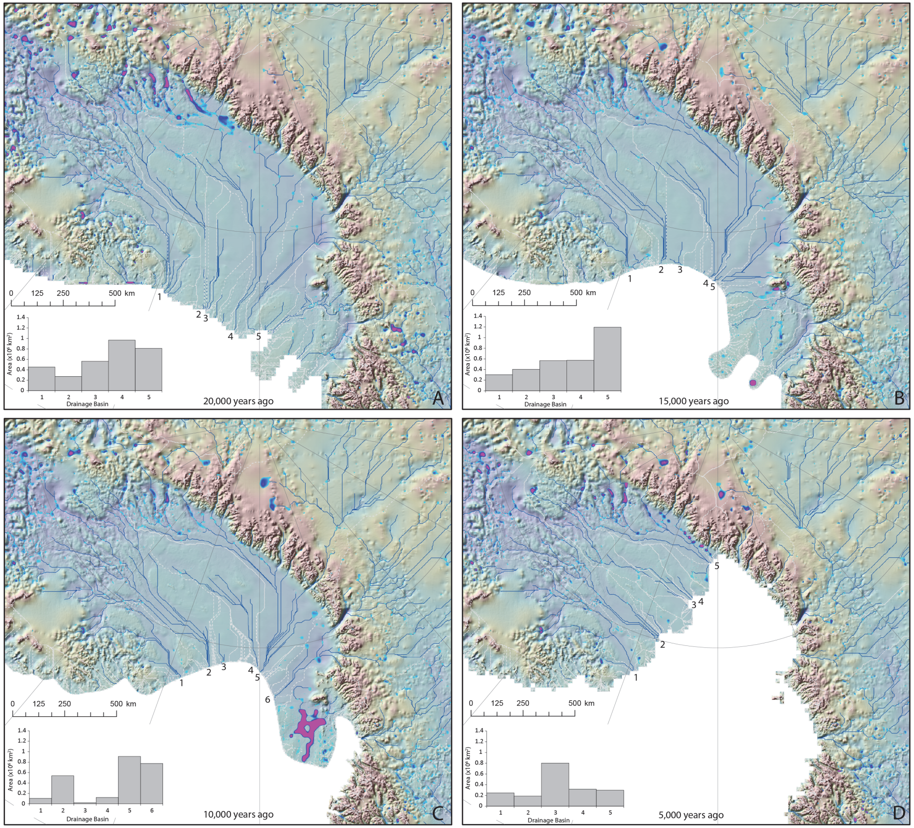

Fig. 3. Simulated subglacial drainage pathways and lakes at 5, 10, 15 and 20 thousand-year timeslices during the deglaciation of the Siple Coast sector of the AIS. The model used is (from Whitehouse et al., 2012). The bar charts illustrate the area of significant drainage basins and correspond to the numbering on the maps. The pale-grey dotted lines divide drainage basins.

TCD
7, 1177–1213, 2013

Predicting subglacial lakes and drainage pathways

S. J. Livingstone et al.

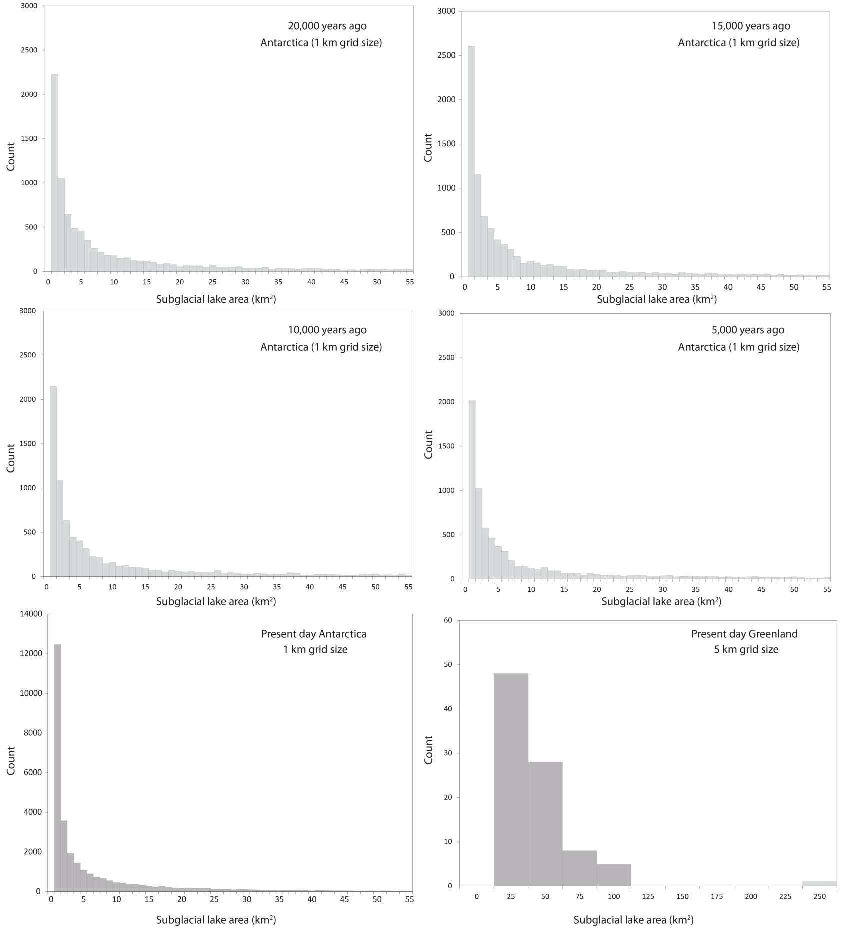

Fig. 4. The distribution of simulated subglacial lake areas. Histograms of Antarctic subglacial lakes are cut at 55 km^2, and Greenland subglacial lakes at 250 km^2.

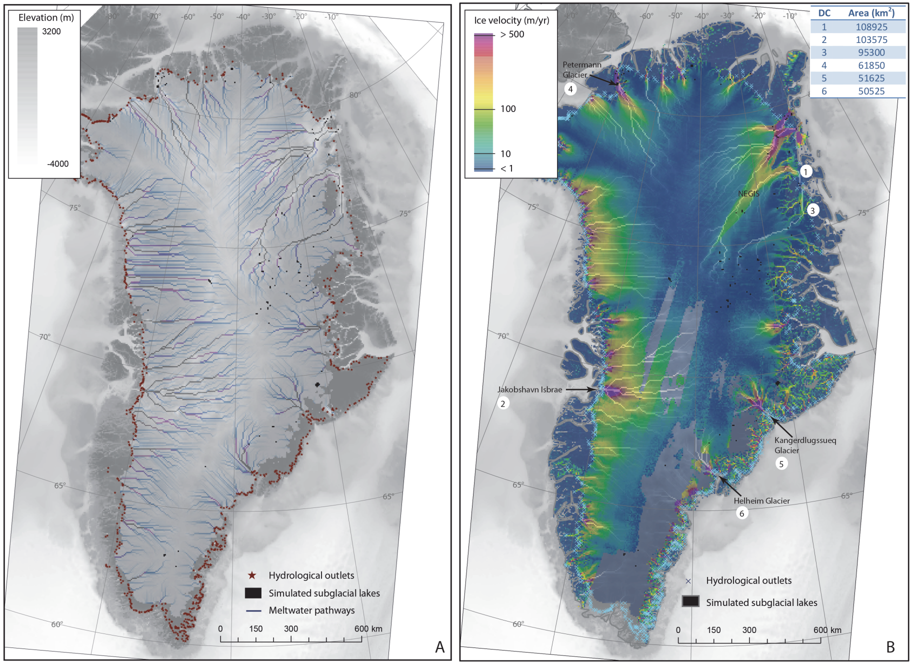

Fig. 5. Simulated subglacial drainage pathways and subglacial lakes beneath the GrIS. **(A)** Illustrates the relationship with bed and ice-surface topographies and observed hydrological outlets (from Lewis and Smith, 2009); and **(B)** illustrates the relationship with ice-surface velocities (Joughin et al., 2010). The six largest drainage catchments (DC) are also listed.

TCD
7, 1177–1213, 2013

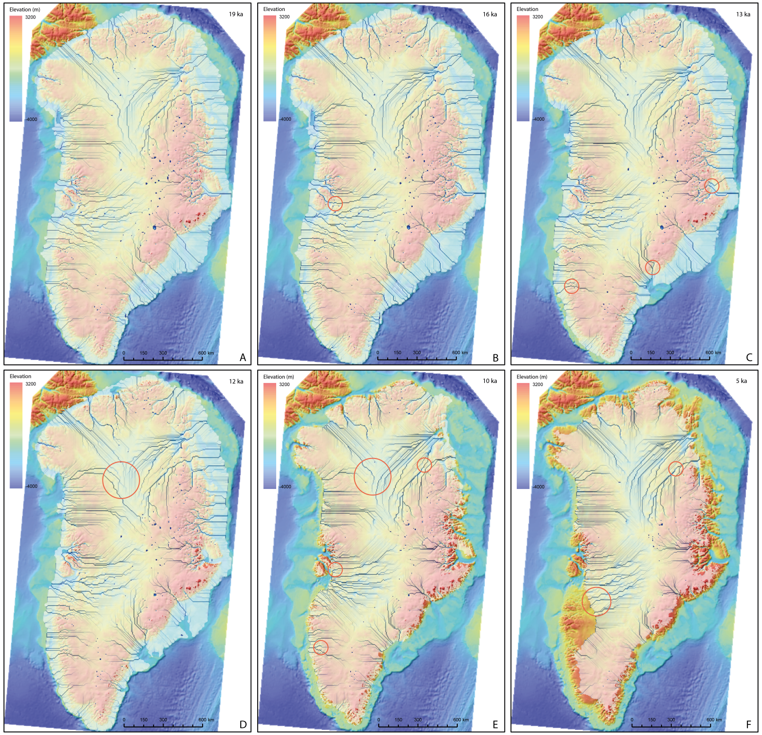

Fig. 6. Simulated drainage networks and subglacial lakes for six time-slices (**A**–**F**) through the evolution of the GrIS since the LGM. Ice-surfaces are derived from Simpson et al. (2009). The opaque white colour delimits the extent of the ice sheet, the blue lines show predicted meltwater pathways and the dark blue colour shows subglacial lake locations. The red circles highlight drainage switches.

TCD

7, 1177–1213, 2013

Predicting subglacial lakes and drainage pathways

S. J. Livingstone et al.

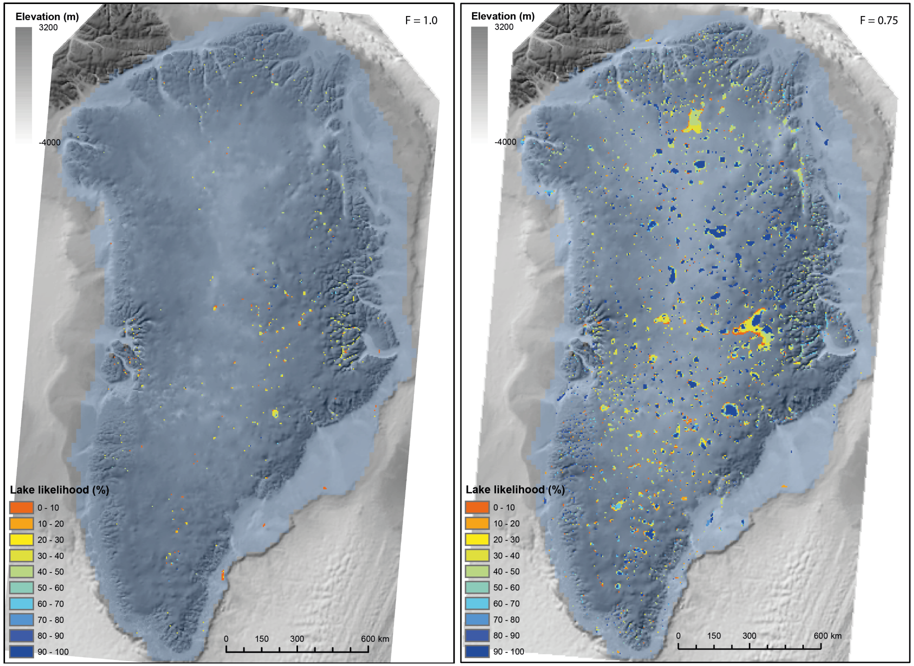

Fig. 7. Subglacial lake likelihood maps for: **(A)** $F = 1$; and **(B)** $F = 0.75$. The likelihood is the percentage time that subglacial lakes occurred in the same location while ice covered that region. Those lakes with a high likelihood are therefore relatively stable.

TCD
7, 1177–1213, 2013

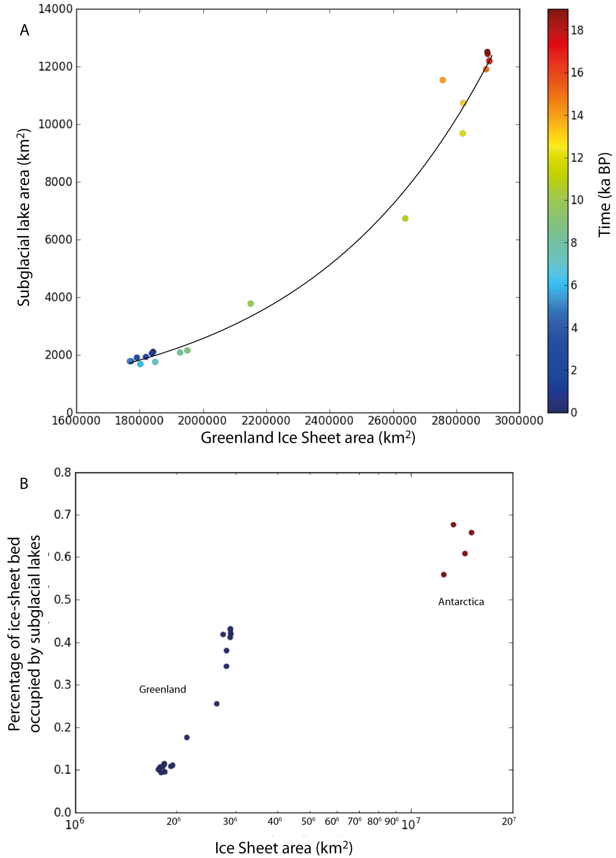

Fig. 8. (A) Scatter graph showing the predicted total subglacial lake area vs. the area of the GrIS and colour-coded according to timeslice (ka); and **(B)** the fraction of the grounded ice-sheet bed occupied by subglacial lakes vs. ice-sheet area, with both the Antarctic and Greenland subglacial lake data plotted. The trend-line in plot A is an exponential curve that generates an R^2 of 0.99.

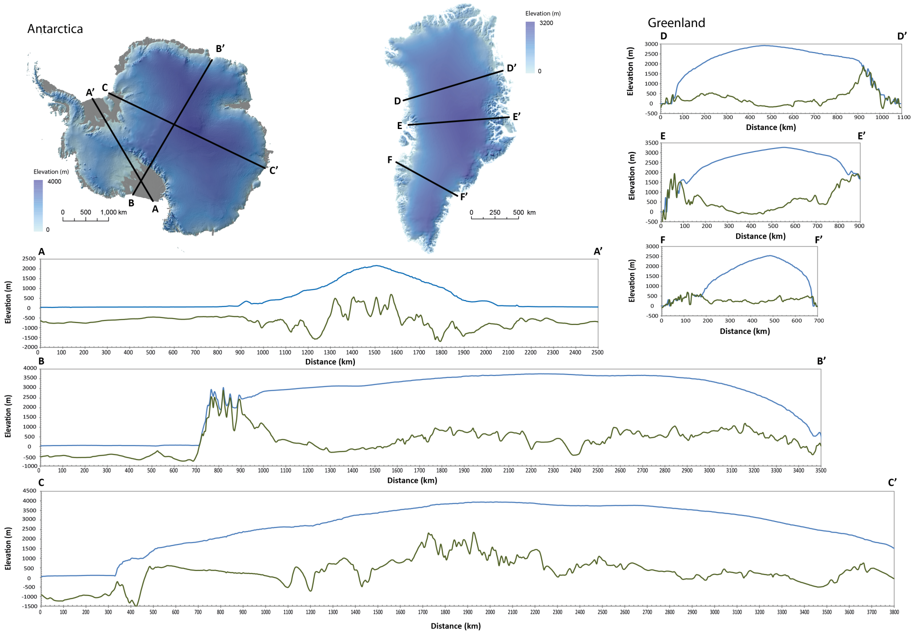

Fig. 9. Bed and ice surface profiles for the Greenland and Antarctic ice sheets. Profiles correspond to the inset images of the two ice sheets and both the vertical and horizontal scales are the same for all profiles. Note how the smaller Greenland Ice Sheet has much steeper overall slopes than the Antarctic Ice Sheet, which because of its size, is characterised by large swathes of relatively flat regions in the interior.

TCD
7, 1177–1213, 2013